Indian J Phys (March 2020) 94(3):391–396
https://doi.org/10.1007/s12648-019-01454-2

ORIGINAL PAPER

Structural phase transition determined from the Bragg angle versus ionization energy plot

A D Arulsamy*

Condensed Matter Group, Institute of Interdisciplinary Science, No. 24, Level-4, Block-C, Lorong Bahagia, Pandamaran, 42000 Port Klang, Selangor DE, Malaysia

Received: 21 July 2018 / Accepted: 05 February 2019 / Published online: 19 April 2019

Abstract: We present here an unexpected relationship to predict the structural phase transition directly and unambiguously from the Bragg angle versus ionization energy plot. We first expose the changes to the F-band optical absorption energy peak in alkali halides so as to justify why the Bragg angle (2θ) versus ionization energy plots for both anions and cations can be used to detect structural phase transition during substitutional doping or systematic changes to chemical composition. In principle, this plot can be extended to predict structural phase transition for all types of solid via doping, which includes cuprates, manganites, topological insulators and cathode materials used in lithium-ion batteries, but, unfortunately, not Fermi metals. The said plot can be implemented in all X-ray diffractometers as an additional feature to predict structural phase transition.

Keywords: Structural phase transition; Bragg angle; Ionization energy

PACS Nos.: 61.05.cp; 61.50.Ah; 61.50.Ks

1. Introduction

In atoms or ions or molecules, we can remove the outer electron from any one of the mentioned species. The minimum energy needed to remove the electron from its original position $\mathbf{r}$ to a distance $\mathbf{r} \to \infty$ is defined as the ionization energy (or the ionization potential in older textbooks) provided that the said electron's kinetic energy remains the same (before and after the removal). Since the energies of bound electrons carry the negative sign, the ionization energies have got to be positive by definition. In solids, the electrons' displacement refers to $r \to r_{\text{finite}}$ where r_{finite} implies the electrons are still bounded within their respective solids. This is one of the foundational principles of the ionization energy theory. The second principle reads—the ionization energy needed to ionize the outer-most electron from atom-1 to a distance $r = r_1$ is proportional to the ionization energy needed to ionize the same electron from atom-1 to a distance $r \to r_\infty$ where obviously $r_1 \ll r_\infty$.

Among the numerous important applications that can be derived unequivocally from the ionization energy theory (IET) [1], which are listed in Ref. [2], we provide here one of the least expected. Based on the above-stated principles, a novel technique is presented here to detect structural phase transition unambiguously in any solid (for as long as they are not Fermi metals) during substitutional doping. The strategy is to first identify the dopant (either a cation or an anion or both) and use their averaged ionization energies plotted against the measured Bragg angle (2θ).

Bragg [3] originally presented a simple derivation and explanation of the diffracted X-ray beams from a crystal in which the incident waves are reflected like a mirror (or specularly) from parallel planes of atoms in a given crystal. Apparently, in Bragg's derivation, the contribution of atomic electrons to the diffracted beams is neglected. Here, we take this effect into account and derive yet another simple relationship between atomic ionization energy (ξ) and the Bragg angle (2θ). However, we note here that Compton was the first one to unambiguously prove (with experimental support) that the scattered wavelength of a scattered X-ray should be larger than that of the incident wavelength, thus establishing the quantum effect in X-ray scattering [4]. Despite the discovery made by Compton,

*Corresponding author, E-mail: sadwerdna@gmail.com

the Compton effect cannot be used to deduce Bragg's angle, 2θ as a function of chemical composition, and therefore, the prediction of structural phase transition from X-ray diffraction is beyond Compton's effect.

Apart from that, it is worth noting that the quantum effect that explains why the scattered wave should depend on the characteristic frequency of a molecule is due to Raman [5–8]. In particular, the characteristic frequency of a molecule mentioned by Raman in 1928 has been proven to be related to the chemical composition of that particular molecule via the atomic energy levels [9], which is also true for solids [10]. On the other hand, the changes to phase and group velocities of a scattered wave, including X-rays, are due to Pancharatnam phase advance [11] in its generalized form, which have been addressed elsewhere [12].

In the following section, we shall provide the necessary physics required to understand why any drastic or sudden change to the Bragg angle implies a drastic change to the averaged ionization energy (ξ) values such that the averaged values used in the plot are no longer valid. In other words, at a certain critical doping where the drastic change occurs, the electronic polarization for the dopant has changed due to the additional contribution made by the polarized core electrons. This in turn gives rise to a structural phase transition that can be observed from the 2θ–ξ plot.

The plot highlighted here can be applied to study the changes to X-ray spectra of doped oxides [13–30], including superconducting cuprates [31, 32], namely, $NdFeAsO_{1-x}F_x$ (x = 0.05 and 0.25) [33], alloys [34, 35] and ferroelectric crystals [36–39]. Moreover, the presence of defects due to multivalent chemical elements such as Fe, V, Mo and Cr in the structurally related $FeVMoO_7$ and $CrVMoO_7$ compounds can also be evaluated as reported by Saritha [40]. These compounds are technologically important as new cathode materials to replace other known compounds in the manufacturing of Li-ion batteries [41–45].

2. Results and discussion

To understand why the ionization energy or the energy-level spacing, ξ, should be able to detect the structural phase transition, we do the following analysis on point defects in alkali halides. The defect known as the *Farbzentrum* or the F-center for short is a type of anion (or negative ion) vacancy defect that has trapped an excess electron, averaged from the nearest-neighbor cations. The German word, *Farbzentrum*, can be translated to read color centers that can be observed from the optical absorption measurement in the visible range [46, 47].

The model based on the trapped electron at the negative-ion vacancy is first suggested by de Boer [46], and much of the earliest experimental work on F-centers was carried out by Pohl [46]. This F-center is the simplest color center with atomic-like optical absorption spectra such that we can neglect other quantum effects that may give rise to complicated optical absorption spectra due to interaction-induced energy-level splitting for the trapped electron. Hence, we can now test the applicability of IET in alkali halides with F-centers. The typical F-bands for several alkali halide crystals can be found in Ref. [46].

The F-band peak decreases from the largest value for LiCl to CsCl where the optical absorption energy for both RbCl and CsCl is 2.0 eV [46], which is due to highly polarized electron because the valence electron from Cs has the lowest or smallest ionization energy. We re-plot these absorption energies for chlorides and other alkali halides as a function of cation's and anion's first ionization energies as displayed in Figs. 1 and 2, respectively. The correlation between the optical absorption energy and the ionization energy is unambiguous, indicated with linear solid lines. More recent data (including simple oxides and sulfides) have been reported in Refs. [48–53] that are also found to obey the notion of ionization energy without any exception. Their relation should be linear because the measured absorption energy is proportional to ξ of the trapped electron.

The trapped electron here of course refers to the outermost valence electron of the cation. The linear relationship is a natural consequence from IET. In particular, for a given anion type, higher cation's first ionization energy implies less polarized valence electron from the cations (or

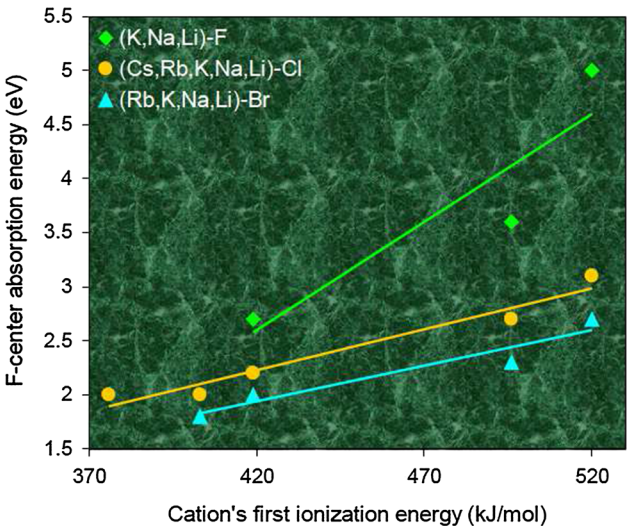

Fig. 1 F-center optical absorption energy as a function of cation's first ionization energy for alkali halides. The linear solid lines here capture the linear proportionality between ξ and optical absorption energy. The experimental data points were obtained from Ref. [46]

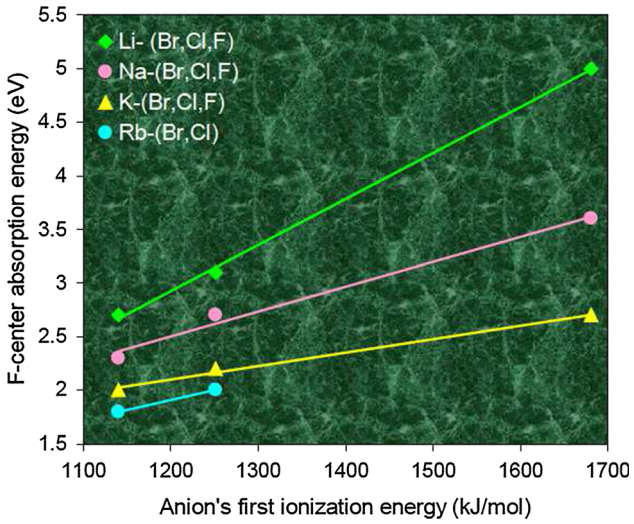

Fig. 2 F-center optical absorption energy versus anion's first ionization energy for alkali halides. The linear solid lines here capture the linear proportionality between ξ and optical absorption energy. The experimental data points were obtained from Ref. [46]

the electron is strongly bounded to the cations), thus increasing the optical absorption energy. Alternatively, for a given cation, if the anion's first ionization energy is increased, then the cation's valence electron is strongly bounded to the anions, leading to the same result—increasing optical absorption energy. This is the precise mechanism responsible to produce the data points depicted in Figs. 1 and 2.

Of course there are missing data especially for Cs halides and alkali iodides, but the fact that both RbCl and CsCl have an identical absorption energy value, 2.0 eV implies the effect of core electron and outer electron polarization from the cations and anions, respectively. For example, the optical absorption energy for CsCl should be smaller than that of RbCl, but this is not the case due to additional polarization from the Cs's core electron that have increased the averaged ξ for Cs, larger than 376 kJ mol^{-1} (see Table 1).

For cases where the change to the Bragg angle (2θ) is small (also due to chemical doping or temperature or applied voltage or electric field), one can still make use of this new plot to evaluate the change to electron polarization where this electron polarization is not large enough to properly initiate any observable or significant structural phase transition. In particular, such small changes to electronic polarization can still be detected from the 2θ–ξ plot as a result of increasing thickness of KY_3F_{10}:Ho^{3+} thin film [54] or due to different annealing temperatures as reported in Ref. [55] for the InGaPN alloy grown on GaAs substrate.

A recent experimental evidence has been reported by Wang et al. [56] using the optical Raman phonon shift

Table 1 Ionization energy values averaged based on a particular ion's valence state

Atoms	Atomic number (Z)	Valence state	Ionization energy (kJ mol^{-1})
Li	3	1+	520†
F	9	1+	1681*
Na	11	1+	496†
Cl	17	1+	1251*
K	19	1+	419†
Br	35	1+	1140*
Rb	37	1+	403†
I	53	1+	1008*
Cs	55	1+	376†

The atoms are listed with increasing atomic number, Z. Each anion is indicated with an asterisk (*), while the cations carry daggers (†), and note that the ionization energies for the cations are always less than that of the anions

where the change to the electronic polarization of individual atoms (especially the ones with the least ionization energies) is the microscopic origin for the structural phase transition, if the said polarization is sufficiently large. In addition, we can also deduce that the electronic polarization-induced structural phase transition is not solely applicable for ferroelectric crystals. For example, rearrangement of electron density due to electronic polarization can cause structural phase transition as a result of chemical doping or temperature or applied voltage (or electric field).

3. Bragg angle versus ionization energy plot: alkali halides

The changes to the peak intensity observed from the peak intensity versus 2θ X-ray diffraction pattern have been correctly formulated by Debye [46], and after applying the energy-level spacing renormalization procedure, the intensity can be derived to read,

$$I(hkl) = I_0 \exp\left\{ -\frac{\hbar|\mathbf{G}|^2}{2M_{\text{ion}}\omega_{\text{ph}} \exp\left[(1/2)\lambda\xi\right]} \right\}, \qquad (1)$$

where $I(hkl)$ and I_0 are the scattered and incident intensity, respectively, hkl are the indices associated with the reciprocal lattice vector, $\mathbf{G}$, $|\mathbf{G}| = G$, M_{ion} denotes ion's mass, and ω_{ph} is the phonon frequency that has been renormalized, which can be done in a straightforward manner. If we remove the exponential renormalizer, Eq. (1) reduces to the standard Debye–Waller intensity formula [46] valid only for absolute zero (T = 0 K) because ω_{ph} without the renormalization factor originates from the zero-point potential energy. After the renormalization, Eq. (1) is valid

for $T > 0$ K (because $\lambda = 1/k_B T$) and for different chemical composition (due to ξ).

The above relation is between ξ and X-ray diffraction intensity. Now, we provide the relevant plots displayed in Figs. 3 and 4 that give the unequivocal experimental evidence for the relation between ξ and 2θ. Before we embark on this proportionality, $\xi \propto 2\theta$, let us first briefly state the interesting aspect of Eq. (1), in which we can use it to correctly predict that when the temperature is increased, the scattered intensity strength or peak intensity, $I(hkl)$, is reduced. On the other hand, $I(hkl)$ achieves a higher peak intensity or value if ξ is larger.

In Refs. [1, 58], the scattering amplitude formula (as functions of scattering angle and ξ) was derived by considering the electron and ion scattering. The scattering amplitude formula is given by [1, 58],

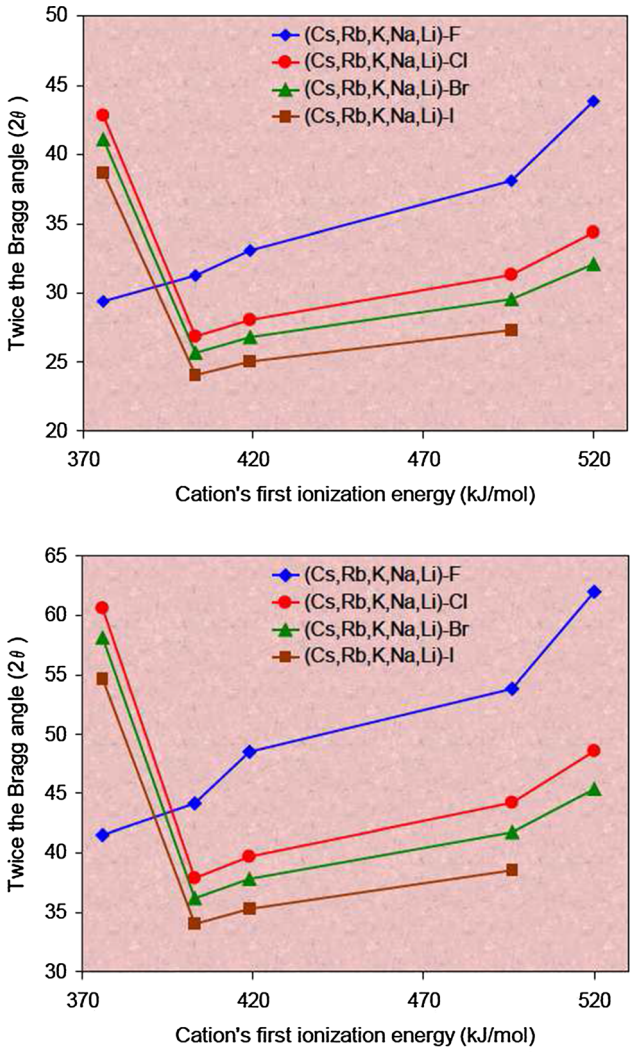

Fig. 3 Cation's first ionization energy is plotted against twice the Bragg angle (2θ) for (200), top diagram, while the bottom diagram is for (220). The solid lines are guides for the eye. The experimental data points were obtained from Ref. [57]

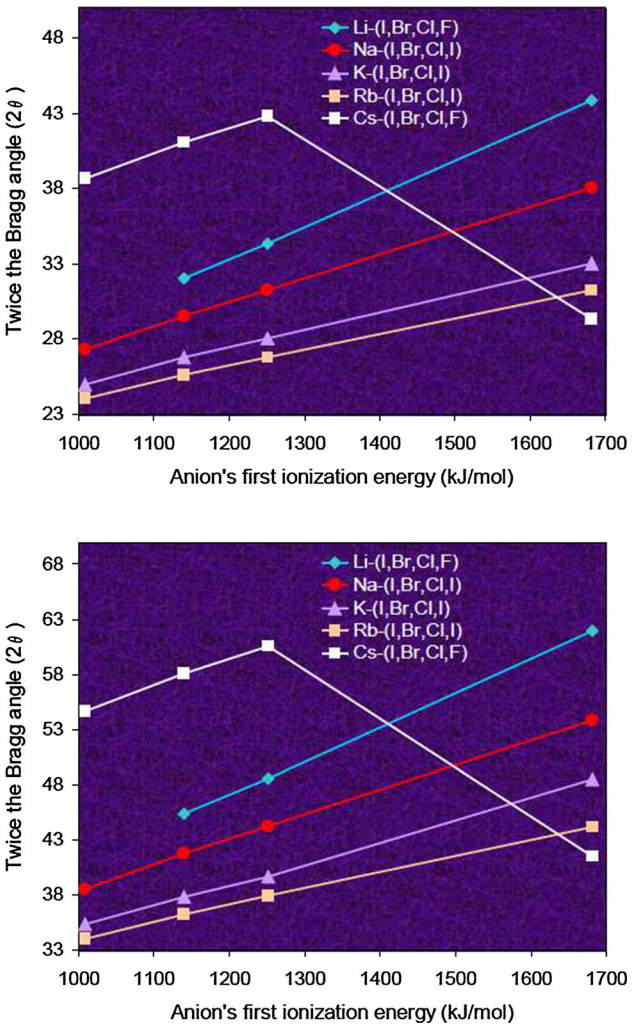

Fig. 4 Anion's first ionization energy versus twice the Bragg angle (2θ) for (200) and (220) plotted in the top and bottom diagrams, respectively. Note that the listed anions should follow in the following order: Na-(I, Br, Cl, F) for all plots. The solid lines are guides for the eye. The experimental data points were obtained from Ref. [57]

$$|f(\theta,\xi)| \propto \frac{1}{\mu_{\mathrm{IET}}^2 \exp(-\lambda\xi) + |\mathbf{k}' - \mathbf{k}|^2}, \tag{2}$$

where μ_{IET} denotes the constant of proportionality with the same unit as the wave vector, $\mathbf{k}$, whereas $|f(\theta,\xi)|$ is a measure of scattering probability for a given θ, and,

$$|\mathbf{k}' - \mathbf{k}| \propto \sin\theta, \tag{3}$$

which denotes the momentum transfer between the incident and the scattered electrons (in strongly correlated solids), and θ is the scattering angle. This θ is caused by the electron-ion scattering, and by definition $\theta = \theta_{\mathrm{el-ion}}$ is inversely proportional to twice the Bragg angle, $2\theta_{\mathrm{Bragg}} = 2\theta$ used in X-ray diffraction data, and therefore, we can redefine Eq. (2) to be compatible for X-ray diffraction by denoting $|\mathbf{k}' - \mathbf{k}|$ as the momentum transfer between the

incident and scattered photons (from X-ray). The scattering center in this case is the cation or an anion. As a consequence, we obtain a simple proportionality between 2θ and ξ,

$$\xi \propto |f(\theta, \xi)| \propto \frac{1}{\theta_{\text{el}-\text{ion}}} \propto \left(\pi - \theta_{\text{el}-\text{ion}}\right) = 2\theta_{\text{Bragg}}. \tag{4}$$

Equation (4) makes perfect physical sense because when $\xi \to \infty$, the system is a classical one with infinitely rigid atoms (with no polarizable electrons) that should give rise to largest possible Bragg angle (depending on the crystal structure). Figures 3 and 4 give remarkable agreement between theory and experiment to the extent that there is no correction needed to understand the plotted data points, and ξ predicts the existence of structural phase transition in alkali halides.

For example, in Figs. 3 and 4, the following alkali halides, CsCl, CsBr and CsI, do not follow the decreasing trend of 2θ with decreasing cation's and anion's first ionization energies. The reason for this is that the crystal structure for the said alkali halides is CsCl, which is different from that of NaCl crystal structure. The NaCl crystal structure is valid for the rest of the alkali halides. In summary, the sudden change in 2θ for decreasing or increasing ξ can be exploited to unambiguously predict the sudden change in the crystal structure or the structural phase transition, induced by the finite-temperature quantum phase transition (due to changing ξ).

Apart from that, the results plotted in Figs. 3 and 4 also provide the strongest experimental support to the claim made in Ref. [1]—the formation of crystal structure (with or without defects) is the effect, not the cause for the many physical properties observed in a given solid. I have excluded the data for LiI because the X-ray data for this particular crystal were obtained using a different radiation with a shorter wavelength, $\lambda = 0.7090$ Å compared to all the other alkali halide crystals.

In summary, 2θ–ξ plot provides an additional and an unambiguous information to identify structural phase transition as well as small changes to electronic polarization (in the absence of structural phase transition). We can obtain the said plot without the need to guess the responsible crystal structures a priori (before and after the structural phase transition) in order to predict the said transition. The traditional method to predict structural phase transition requires one to know the crystal structures a priori (before and after the structural phase transition) in order to calculate its lattice parameters and the sudden change in the lattice parameters. In particular, the prediction of structural phase transition using this commonly employed traditional method of utilizing the change in the lattice parameters (or crystal structure volume) is still being exploited as the primary method [15, 33], which can be further substantiated and supported with 2θ–ξ plot.

4. Conclusion

In conclusion, we have established an accurate relationship between the Bragg angle and the averaged ionization energy of different chemical elements in alkali halides. After doing so, we have moved on to exploit the said relationship to plot the Bragg angle (2θ) versus ionization energy (ξ). Subsequently, we proved that any large deviation detected from the usual trend in this 2θ–ξ plot should indicate a type of structural phase transition or crystal structure transformation. We have shown that this conclusion should not be surprising from the standard theory of X-rays with respect to Debye–Waller factor, which has been renormalized in our theory presented above. For example, the change in the electronic polarization (of valence electrons) influences the atomic form factor, which in turn leads to a corresponding change in the structure factor. In principle, we should be able to use this plot to study the structural phase transition (major or minor) in other complex and technologically important materials, namely, in cuprate and pnictide superconductors, ferromagnetic manganites and semiconductors, inorganic and oxide semiconductors, Mott insulators, topological insulators and the solid materials used in Li-ion batteries, provided that these materials are not in the same league as Fermi metals.

Acknowledgements This work was supported by Sebastiammal Savarimuthu and the late Arulsamy Innasimuthu (1941–2017).

References

[1] A D Arulsamy *Ionization Energy Theory: Formalism* (Seattle : CreateSpace) (2016)
[2] A D Arulsamy *Ionization Energy Theory II: Interdisciplinary Science* (Seattle : CreateSpace) (2017)
[3] W L Bragg *Proc. Camb. Phil. Soc.* **17** 43 (1913)
[4] A H Compton *Phys. Rev.* **21** 483 (1923)
[5] C V Raman *Indian J. Phys.* **2** 387 (1928)
[6] C V Raman and K S Krishnan *Indian J. Phys.* **2** 399 (1928)
[7] C V Raman and K S Krishnan *Nature* **121** 501 (1928)
[8] C V Raman *Nature* **121** 619 (1928)
[9] A D Arulsamy *Indian J. Phys.*https://doi.org/10.1007/s12648-019-01394-x (2019)
[10] A D Arulsamy *Phys. Scr.* **94** 055803 (2019)
[11] S Pancharatnam *Proc. Indian Acad. Sci. A* **44** 247 (1956)
[12] A D Arulsamy *Optik*https://doi.org/10.1016/j.ijleo.2018.11.061 (2019)
[13] J Rout and R N P Choudhary *Indian J. Phys.* **92** 575 (2018)
[14] R V K Mangalam and A Sundaresan *J. Chem. Sci.* **99** 118 (2006)
[15] U Farid, H U Khan, M Avdeev, S Injac, *J. Solid State Chem.* **258** 118 (2018)
[16] A Jafari, S F Shayesteh, *Indian J. Phys.* **89** 551 (2015)

[17] W B Aribia, M Abdelmouleh, *J. Chem. Sci.* **124** 403 (2012)
[18] S Raju and E Mohandas *J. Chem. Sci.* **122** 83 (2010)
[19] R M Sebastian and E M Mohammed *Indian J. Phys.* **90** 1397 (2016)
[20] D S V Thampi, *J. Solid State Chem.* **255** 121 (2017)
[21] C Xing, J Li, H Chen, H Qiao, J Yang, H Dong, H Sun, J Wang, X Yin, Z M Qi and F Shi *RSC Adv.* **7** 35305 (2017)
[22] H Qiao, H Sun, J Li, H Chen, C Xing, J Yang, H Dong, J Wang, X Yin, Z M Qi and F Shi *Scientific Rep.* **7** 13336 (2017)
[23] D Roy, S Mandal, C K De, *Phys. Chem. Chem. Phys.* **20** 13336 (2018)
[24] W B H Othmen, *Mater. Sci. Semicond. Process.* **52** 46 (2016)
[25] W Li, X Wu, J Chen, Y Gong, *Sens. Actuat. B* **253** 144 (2017)
[26] B Sambandam, T Muthukumar, S Arumugam, P L Paulose and P T Manoharan *RSC Adv.* **4** 22141 (2014)
[27] A N Radhakrishnan, P P Rao, S K Mahesh, *Inorg. Chem.* **51** 2409 (2012)
[28] B Sambandam, S E Muthu, S Arumugam and P T Manoharan *RSC Adv.* **3** 5184 (2013)
[29] D S V Thampi, P P Rao and A N Radhakrishnan *RSC Adv.* **4** 12321 (2014)
[30] S Kaniyankandy, *J. Mater. Chem.* **C1** 2755 (2013)
[31] A Ricci, N Poccia, *J. Supercond. Nov. Magn.* **24** 1201 (2011)
[32] S Margadonna, Y Takabayashi, M T McDonald, M Brunelli, G Wu, R H Liu, *Phys. Rev.* **B79** 014503 (2009)
[33] M Calamiotou, D Lampakis, N D Zhigadlo, S Katrych, J Karpinski, A Fitch, P Tsiaklagkanos and E Liarokapis, *Phys. C: Supercond. Appl.* **527** 55 (2015)
[34] N V Chandra Shekar, V Kathirvel and P Ch Sahu *Indian J. Phys.* **84** 485 (2010)
[35] F Oumelaz, O Nemiri, A Boumaza, S Ghemid, H Meradji, *Indian J. Phys.* **92** 705 (2017)
[36] R A Cowley and S M Shapiro *J. Phys. Soc. Jpn.* **75** 111001 (2006)
[37] F Jona and G Shirane *Ferroelectric Crystals* (Oxford : Pergamon Press) (1962)
[38] G Shirane *Rev. Mod. Phys.* **45** 437 (1974)
[39] M Fujimoto *The Physics of Structural Phase Transitions* (Berlin : Springer) (2005)
[40] D Saritha *J. Chem. Sci.* **130** 7 (2018)
[41] S R S Prabaharan, *Electrochem. Solid-State Lett.* **7** A416 (2004)
[42] K M Begam, M S Michael, *Electrochem. Solid-State Lett.* **7** A242 (2004)
[43] K M Begam and S R S Prabaharan *J. Power Sources* **159** 319 (2006)
[44] A Manthiram and J B Goodenough *J. Power Sources* **26** 403 (1989)
[45] S R S Prabaharan, M S Michael, *J. Electroanal. Chem.* **570** 107 (2004)
[46] C Kittel *Introduction to Solid State Physics* (New York : Wiley) (1976)
[47] J H Schulman and W D Compton *Color Centers in Solids* (Oxford : Pergamon) (1962)
[48] A I Popov, *Nucl. Instr. Meth. B* **268** 3084 (2010)
[49] M P Tosi *Solid State Phys.* **16** 1 (1964)
[50] L Frevel *Ind. Eng. Chem. Anal. Ed.* **14** 687 (1942)
[51] R K Dowson and D Poole *Phys. Status Solidi* **35** 95 (1969)
[52] E A Kotomin and A I Popov *Nucl. Instr. Meth. B* **141** 1998 (1998)
[53] R Pandey, *J. Mater. Res.* **3** 1362 (1988)
[54] N Gemechu and T Abebe *Ukr. J. Phys.* **63** 182 (2018)
[55] P Sritowong, *Ukr. J. Phys.* **63** 276 (2018)
[56] Y Wang, J Xiao, H Zhu, Y Li, Y Alsaid, K Y Fong, Y Zhou, S Wang, W Shi, Y Wang, A Zettl, E J Reed and X Zhang *Nature* **550** 487 (2017)
[57] D B Sirdeshmukh, L Sirdeshmukh and K G Subhadra *Alkali Halides: A Handbook of Physical Properties* (Berlin : Springer) (2001)
[58] A D Arulsamy *RSC Adv.* **6** 109259 (2016)